Atomic defects in titanium dioxide.

AUTHOR(S):

Minato, Taketoshi

Atomic Defects in Titanium Dioxide

Taketoshi Minato

Office of Society-Academia Collaboration for Innovation,

Kyoto University, Gokasho, Uji,Kyoto 611-0011 (Japan)

E-mail: minato.taketoshi.5x@kyoto-u.ac.jp

ABSTRACT: The functionality of solid materials is defined by the type and ordering of the constituent atoms. By introducing defects that perturb the ordered structure, new functionality is created within the solid material. Atomic defects in titanium dioxide, such as oxygen vacancies, atomic hydrogen, and interstitial Ti, typically create new functionality. However, the fundamental physical properties of atomic defects in TiO_2 are not fully understood and still remain controversial. In this account, the progress and issues for debate regarding the physical properties, electronic structure, and manipulation mechanisms of atomic defects in TiO_2 as well as their interaction with gold nanoclusters are described.

Keywords: defects, electronic structure, solid-state structures, surface analysis, titanium dioxide

1. Introduction

The functionality of solid materials is determined by the type and ordering structure of their constituent atoms. The introduction of perturbations in the structure of a material often drastically changes the functionality of the material. For instance, atomic defects on the surface of titanium dioxide (TiO_2) result in changes in its functionality. TiO_2 is used widely for catalysis, photocatalysis, the conduction of electrons/holes/ions, as a sensing material in photoelectrolysis, and for inducing photoinduced superhydrophilicity. Furthermore, TiO_2 is also used as a pigment, a cosmetic, a food additive, a filler in pills, a scattering agent for ultraviolet (UV) light, and a sterilizer. It has been reported that atomic defects such as oxygen vacancies, atomic hydrogen (hydroxyl), and interstitial Ti have a marked effect on the functionality of TiO_2. However, the mechanisms underlying the changes in this functionality are not yet fully understood. Thus, clarification of the fundamental physical properties of atomic defects is necessary to understand these mechanisms.

In this account, I will describe the current knowledge and issues of debate on the physical properties of atomic defects in TiO_2. The electronic structure, the manipulation mechanisms of atomic defects, and the interaction with gold nanoclusters are selected as the topics in this account because they are fundamentally important and controversial topics. Investigations based on surface science techniques such as scanning tunneling microscopy (STM) and photoelectron spectroscopy (PES) performed in ultrahigh vacuum (UHV) are mainly discussed this account.

The increase in the number of studies related to atomic defects in TiO_2 is evidence of the interest in the subject. The black curve in Figure 1 indicates the number of publications *N(TiO$_2$ and defect)*, including research articles, letters, and reviews,

corresponding to the keywords "TiO_2" and "defect". This number, which was calculated using a system provided by the Web of Science™ platform,[1] reflects the number of publications since 1959. As observed from the curve, the number of publications was not high up to 1990, and only five publications were published in 1990. Starting in 1991, the number of publications has increased gradually. In 2013, the number of publications was 73.4 times (367 publications) higher than that in 1990. To determine the effect of this increase with respect to the total number of publications in all journals, we calculated the following value:

$$\frac{N(TiO_2 \text{ and defect})}{N(\text{total})}$$

where *N(total)* is the total number of publications in all journals, as determined using our search system of the Web of Science™ platform. The blue curve in Figure 1 is a plot of the aforementioned value for different years. It can be seen that this value has also increased significantly since 1991. This clearly indicates that research interest in atomic defects on TiO_2 surfaces is increasing. The elucidation of the physical properties of TiO_2 using surface science techniques most likely also contributed to this increase in interest. Previous knowledge regarding the physical properties of atomic defects in TiO_2 has been summarized in multiple reviews (Table 1).[2–15] This account describes the recent progress and issues of debate for elucidating the physical properties of the atomic defects in TiO_2.

2. Structure of Atomic Defects in TiO_2

Figure 2 shows the structures of the following atomic defects on the rutile TiO_2(110) surface, which is the most widely investigated TiO_2 surface type: a bridging oxygen vacancy (O_{bvac}), atomic hydrogen (H_a), and interstitial Ti (Ti_{int}). Historically, O_{bvac} has been believed to be the primary defect and related to the functionality of this TiO_2 surface. Wendt *et al*. and Bikondoa *et al*. reported that O_{bvac} reacts readily with residual water, even under UHV conditions.[16,17] The reaction produces two H_a defects on the surface.[16–18] In reactions involving photocatalysis, photoelectrolysis, and photoinduced superhydrophilicity, all O_{bvac} vacancies would be filled with water. Furthermore, it has been recently reported that Ti_{int} exists at the subsurface and plays an important role in functionality on the TiO_2 surface. Previously, Aono and Yagi *et al.* suggested that Ti_{int} exists in the bulk of rutile TiO_2 and affects electron conduction.[19,20] Furthermore, Henderson suggested that Ti_{int} is the key point defect in reduced TiO_2.[21] In 2008, Wendt *et al*. reported that subsurface Ti_{int} in rutile TiO_2 can interact with adsorbates on the surface.[22] Currently, it is generally believed that Ti_{int} has an important role in the functionality on the TiO_2 surface as well as O_{bvac} or H_a.[23–46]

Oxygen vacancies and atomic hydrogen tend to exist on the surface rather than in the bulk of rutile TiO_2(110). STM images obtained under positive sample biasing conditions show that O_{bvac} and H_a exhibit similar protrusions towards the row of the bridging oxygen (O_b) atoms (Figure 3).[16,17,47–51] In addition, frequency-modulated atomic force microscopy (FM-AFM) has shown that O_{bvac} and H_a occur as depressions in the O_b row.[52,53] The protrusions in the O_b rows observed in STM images obtained under a positive sample bias were assigned to O_{bvac}[54] because it is generally believed that O_{bvac} exists on the surface. Later, it was found that residual water reacts readily

with O_{bvac},[16,17] and O_{bvac} is filled by the products of water dissociation in many cases. Furthermore, it was revealed that O_{bvac} and H_a in STM images under positive sample biasing conditions are similar.[16,17] In some cases, the assignment of the protrusions in the O_b rows in the STM images under positive sample bias is changed to H_a.[55] It is now possible to distinguish O_{bvac} and H_a in STM images obtained under a positive sample bias from their apparent heights (that of H_a is slightly greater) and responses to high-bias-voltage stimulation

(H_a undergoes desorption, and O_{bvac} undergoes lateral diffusion).[16,17,47–51]

The direct observation of Ti_{int} by STM and FM-AFM is not possible because it exists at the subsurface. For STM imaging of Ti_{int}, the adsorption of oxygen molecules on the surface allows Ti_{int} to diffuse to the surface. Ti_{int} reacts with the oxygen molecules, and this can be observed from the higher protrusions in the STM images (Figure 4).[22] By using transmission electron microscopy (TEM), Shibata *et al.*[23] and Tanaka *et al.*[45] directly observed Ti_{int}.

3. Electronic Structures of Defects

The functionality of TiO_2 is affected by the introduction of defects. The electronic structures of the defects on TiO_2 surfaces have been investigated extensively. TiO_2 has a band gap of 3.1 eV, and the introduction of atomic defects modifies the electronic structure in the band gap, forming band-gap states (BGSs). Although numerous studies have been performed on BGSs, their true nature is not yet fully understood. In particular, the spatial distribution and origin of the BGSs have been widely investigated recently; however, they are controversial. In this section, the controversy regarding the electronic structures of the BGSs induced by atomic defects is described.

3.1. Spatial Distribution of Band-Gap States

I begin by discussing the BGSs induced by O_{bvac}. The removal of a single neutral oxygen atom from TiO_2 results in two excess electrons in the material. These electrons occupy the energetically lowest state, mainly formed by the Ti 3d state.
The occupation of the Ti 3d state creates a BGS. The spatial distribution of the BGSs is of fundamental importance; however, it is still controversial.

In a study based on PES, Henrich *et al*. showed that the BGSs were created at approximately 1 eV below the Fermi level in reduced rutile TiO_2(110).[56] X-ray photoelectron spectroscopy (XPS) has shown that Ti^{3+} exists on the surface of TiO_2, suggesting the localization of the excess charge at Ti sites.[57] On the basis of these results, it was proposed that a BGS is localized at Ti_{6c} under O_{bvac}. Later, numerous studies were reported on the localization of defect states. A study based on angleresolved PES (ARPES) (Figure 5) showed that the BGSs were not dispersed.[58]

Furthermore, the results of theoretical calculations of the electronic structure of O_{bvac} suggested that the BGSs were localized at the Ti sites.[59–61] However, several other reports have stated that the BGSs are delocalized in TiO_2.[62–64] Henderson *et al*. discussed the effects of the delocalization of an extra electron around O_{bvac} on oxygen dissociation.[65]

By using STM and scanning tunneling spectroscopy (STS), we directly observed the spatial distribution of BGSs at the atomic scale.[47] Previously, STM observation of TiO_2 reported on positive sample bias conditions because TiO_2 becomes an n-type semiconductor, and the unoccupied states are close to the Fermi level after TiO_2 is cleaned by annealing and ion sputtering. Via the detection of a small density of the occupied states, we successfully observed occupied-state images of TiO_2. Figure 6 shows the simultaneously obtained images of the unoccupied (V_{sample} = +0.6 V) and occupied (V_{sample} = −1.1 V) states at O_{bvac} sites at 78 K. The STM images clearly show that the BGSs are not atomically localized; however, they are distributed around Ti_{5c}. The STS spectra of Ti_{5c} also showed BGSs at approximately -0.9 V (Figure 7).

From these direct observations, we proposed that the BGSs are not atomically localized but distributed on several Ti_{5c} sites. Using resonant photoelectron diffraction analysis, Krüger *et al*. found that extra electrons are present in a wide distribution around the Ti_{5c} ions, which surround the O_{bvac} sites.[66] On the other hand, it has been suggested that BGSs are localized around O_{bvac} by using STM current imaging tunneling spectroscopy (CITS)-based mapping at liquid helium temperatures.[67] Furthermore, studies based on the theoretical calculations of the electronic structure of O_{bvac} have also reported that the BGSs are localized.[68] It has been proposed that a delocalized feature is observed when using STM due to the temperature during observation, because the polaron mobility is

high at this temperature.[69,70] On the other hand, the recent results of density functional theory (DFT) calculations performed by Cai *et al*. suggest that the defect states have a wide distribution in TiO_2.[71]

The situation for the investigation of the electronic structure induced by H_a is similar to that of O_{bvac}. A H atom on O_b gives electrons to TiO_2 with local distortion. The transferred electrons occupy the lowest energy states of TiO_2 that are mainly formed by the Ti 3d states of Ti_{5c}.[61] We have observed the spatial distribution of BGSs induced by H_a by occupied state STM at 78 K and proposed that the BGSs are not atomically localized and distributed on the Ti_{5c} sites as well as O_{bvac} (Figure 8).[47] The weaker occupation of electrons at the Ti 3d states than at O_{bvac} was also observed for H_a.[47] On the other hand, Papageorgiou *et al*. suggested that the BGSs induced by H_a are localized on the basis of CITS mapping data at liquid helium temperatures.[67]

The spatial distribution of the BGSs induced by Ti_{int} is still unclear. This is due to a lack of direct observation of the electronic structure induced by Ti_{int} at the subsurface by microscopic techniques. DFT calculations showed that the spatial distribution of the BGSs induced by Ti_{int} is widely distributed.[24,46]

Thus, as described above, the nature of the spatial distribution of the BGSs remains a topic of debate, and further investigations are necessary to end this controversy. It is generally accepted that the use of hybrid functionals or GGA+U in theoretical calculations produces BGSs that are spatially localized.[47,61,69,70] In contrast, the use of non-hybrid functionals has shown that they are spatially delocalized.[47,61,63] However, the distribution of the defect states in the bulk or subsurface regions can be experimentally determined by direct observation using microscopy techniques. The development of experimental techniques that allow for the direct observation of the

electronic structure of defects including those in the bulk and subsurface regions would be necessary for resolving the debate surrounding this issue.

3.2. Origin of the Band-Gap States

For a long time, it was believed that oxygen vacancies played an important role in the formation of BGSs. However, recent reports regarding the BGSs suggested that oxygen vacancies and other defects both contribute to the BGSs.

In an early study based on PES results, Henrich *et al*. showed that the BGSs were created at approximately 1 eV below the Fermi level in reduced rutile TiO_2(110) by annealing in UHV or Ar^+ sputtering.[56] Because O_{bvac} was believed to be the main defect in rutile TiO_2(110), the origin of the BGSs was assigned to the contribution of O_{bvac}. The assignment of the BGSs to O_{bvac} was believed to be correct and was used for the interpretation of the functionality of TiO_2. The STM work by Wendt *et al*. and Bikondoa *et al*. clarified that O_{bvac} does not exist in many previous experiments.[16,17] Therefore, the origin of the BGSs had to be reconsidered. In 2006, Di Valentin *et al*. showed that both O_{bvac} and H_a create BGSs by DFT calculations.[61]

In 2008,Wendt *et al*. reported that Ti_{int} has contributions to the BGSs on the basis of STM, PES, and DFT calculations.[22] DFT calculations of the electronic structure of Ti_{int} performed by other groups also showed that Ti_{int} creates BGSs.[24,29,46] These works suggested that the O_{bvac}, H_a, and Ti_{int} defects have to be considered for the contribution to the BGSs. In fact, Wendt's conclusion was that Ti_{int} is almost the only source of BGSs.[22] This is entirely in contrast to the previously believed model that states that O_{bvac} and H_a are the main sources of BGSs. However, the contribution of Ti_{int} to the BGSs is still controversial, and recent reports have shown that the contribution of

Ti_{int} to the BGSs is not as large as O_{bvac} or H_a. For example, our STM/STS results (Figures 6–8) showed that O_{bvac} and H_a are the sources of BGSs, even though they do not exclude the contribution of Ti_{int}.[47] This is not in agreement with the conclusion that Ti_{int} is the only source of BGSs. Direct evidence of the small contribution of Ti_{int} to the BGSs was reported by Yim *et al*. They showed a linear relationship between the density of O_{bvac} and the intensity of the BGSs via the combined use of STM and PES (Figure 9).[72] Interestingly, it was concluded that a small portion of the BGSs is attributable to other defects such as Ti_{int} by extrapolating the experimental results. Furthermore, Mitsuhara[73] and Walle[74] also showed that both O_{bvac} and Ti_{int} are related to the BGSs. The O_{bvac} sites contribute more to the formation of BGSs than Ti_{int}.[73] Moreover, Mao *et al*. showed that H_a has a major contribution to the BGSs as well as O_{bvac} on the basis of PES and DFT results, and the contribution of Ti_{int} is smaller than H_a.[46]

As described above, the origin of the BGSs is still not fully understood. The three types of defects, O_{bvac}, H_a, and Ti_{int}, have contributions to the BGSs,[75] although the relative contribution is not the same. In order to accurately evaluate the contribution of each atomic defect to the BGSs, further conclusive studies are required. For example, the contribution of each defect could be determined by a comparison of the intensity of the BGSs with three TiO_2 samples each having the same density of one of the three defects. In addition, direct observation of the electronic structure induced by Ti_{int} would be ideal to determine the contribution of Ti_{int} to the BGSs; however, this has not been achieved yet because the observation of the electronic structure induced by Ti_{int} at the subsurface is not possible by conventional microscopy techniques such as STM. The development of experimental techniques to directly observe the electronic structure in the subsurface or bulk would be required.

4. Manipulation of Defects

The physical properties of TiO_2 are strongly affected by atomic defects. The control of the densities and surface alignments of atomic defects would result in new functionality of TiO_2. The introduction of defects was carried out by annealing in vacuum; this induced oxygen molecules to desorb from the surface and produce an oxygen vacancy.[56] Furthermore, Ar^+ sputtering was used to reduce TiO_2.[56] In 1978, Knotek and Feibelman reported the photo- and electron-stimulated desorption of oxygen ions via an interatomic Auger decay process.[76] The Knotek–Feibelman (K–F) process is a typical process for inducing ionic desorption via photon and electron excitation. Zhang *et al*. reported the effects of the spreading of defect electrons on the desorption of oxygen from a TiO_2 surface.[77]

Recently, the control of the alignment of defects at the atomic scale (i.e., their manipulation) was achieved using STM. The methods for manipulating atoms/molecules using STM can be separated into two categories: electron-excitation processes and non-electron-excitation processes. In electronexcitation reactions, three excitation mechanisms have been proposed. Tunneling electrons excite electronic states related to chemical bonds (electronic-state excitation).[78] The electrons could also be excited into electronic states related to vibrational states, including translational, rotational, and conformational change states (vibrational-state excitation) to overcome reaction barriers by exciting reaction coordinate modes.[79–81] Furthermore, heating by electrons also caused reactions owing to electron excitation (manipulation by local heating).[82] In nonelectron-excitation reactions, direct interactions between the STM tip and the atoms/molecules due to the van der Waals/chemical forces (direct manipulation)[83] or an electric field to reduce the height of the reaction barrier (electric-

field excitation) are exploited to manipulate atoms/molecules.[84–86] Even though the underlying mechanisms are not always known, these techniques can be used to control the alignment of atomic defects on TiO_2 surfaces.

The manipulation of defects on rutile TiO_2(110) surfaces was first reported by Diebold *et al*. in 1998.[87] They observed the disappearance of defects when scanning at V_{sample} = +3.0 V and attributed this phenomenon to the movement of oxygen atoms between the tip and the O_{bvac} sites on the surface. Later, Suzuki *et al*. clarified that this movement was due to the desorption of H_a on the surface (Figure 10).[49] The mechanism of the desorption of H_a was studied by Acharya *et al*., and they proposed that this reaction was induced by the vibrational excitation of the O–H stretching mode.[88]

The manipulation of defects on rutile TiO_2(110) surfaces using an STM tip to allow for the in-plane diffusion of O_{bvac} has also been reported. For instance, Diebold *et al*. reported the diffusion of O_{bvac} on a TiO_2 surface.[87] Cui *et al*. reported the diffusion of a single O_{bvac} induced by excitation from an STM tip.[89] Using this method, they were able to form pairs of O_{bvac}; such pairs are rarely observed on surfaces prepared by cycles of Ar^+ sputtering and subsequent annealing. The diffusion of these pairs of O_{bvac} has also been reported.[89] The excitation mechanism of this reaction is not known; however, the application of a high bias voltage is necessary for the reaction to take place. This suggests that the electric field between the tip and the surface plays an important role in the reaction.

In addition, we reported that oxygen desorption (i.e., the creation of O_{bvac}) could occur by applying a negative sample bias from the STM tip (Figure 11).[50] This reaction is only possible when the applied sample bias is negative. This result also suggests that

the ability to manipulate the defects on a TiO_2 surface is related to the electric field between the tip and the sample surface (Figure 12).[50] TiO_2 is composed of titanium and oxygen (and adsorbed hydrogen) ions. The modification of the electronic structure of these ions by an applied electric field plays a key role in the excitation process that results in the manipulation reactions.

In contrast, the introduction of oxygen vacancies to the anatase TiO_2(101) surface can be achieved by applying a positive sample bias, which induces the migration of oxygen vacancies from the subsurface region to the surface.[90] It has been suggested that the applied electric field has an effect on the migration of oxygen vacancies. The mechanism underlying the differences between rutile TiO_2(110) and anatase TiO_2(101) is still unclear.

5. Interaction of Defects with Gold Nanoclusters

TiO_2 has been widely used as a support for metal catalysts. One of the early uses of TiO_2 was to disperse expensive precious metals over a high surface area (small particle size). Later, it was found that the electronic interaction between TiO_2 and the metals influenced the catalytic behavior.[2–15,91] In particular, the BGSs, which are located near the Fermi level, strongly interact with the metal; thus, they are considered to have an important role in the support–metal interaction. Recently, the effects of the BGSs on the catalytic activity have attracted much attention for the activation process of Au nanoclusters. Au is a chemically stable metal; however, Haruta *et al*. discovered that Au nanoclusters (2–3 nm) supported on TiO_2 (or other supports) exhibited a significantly high activity for CO oxidation at room temperature.[92,93] Among the numerous reports on the activation mechanism of Au nanoclusters, the interaction of the BGSs is believed to have an important role.[93,94] In this section, the recent progress related to the roles of the BGSs for the activation of Au nanoclusters is described.

One of the most important issues of the interaction between BGSs and Au nanoclusters is the electron transfer to change the charge state of Au. Early studies on work function measurements of Au/TiO_2 showed that electrons are transferred from the supported Au nanoclusters to TiO_2; thus, the Au nanoclusters are positively charged on TiO_2.[95] In contrast, DFT calculations for Au adsorbed at O_{bvac} on TiO_2 showed electron transfer from TiO_2 to Au.[63] On the other hand, DFT calculations by Wahlstrom *et al*. showed that the electron transfer is not large between Au and TiO_2 with O_{bvac}.[96] Therefore, the charge state of a Au nanocluster supported on TiO_2 has not been elucidated.

We performed PES on reduced TiO_2 with different Au coverages and found that there is a clear shift in the energy of the O 2p states (Figure 13) and a decrease in the BGSs (Figure 14).[97] The change in the spectra according to the amount of Au deposited is attributed to the electron transfer from TiO_2 to the Au nanoclusters. This clearly showed that the Au nanoclusters supported on reduced TiO_2 are negatively charged. Later, the negative charge of the Au nanoclusters on reduced TiO_2 was confirmed via vibrational spectroscopic study of CO molecules adsorbed onto Au/TiO_2.[98,99] The facilitation of CO oxidation on negatively charged Au nanoclusters was concluded by the DFT calculations of several groups.[100–104] In addition, Kelvin probe force microscopy (KPFM) observation of the charge state of the Au nanoclusters on reduced TiO_2 directly revealed that the Au nanoclusters are negatively charged (Figure 15).[105] Therefore, the Au nanoclusters supported on reduced TiO_2 are negatively charged, which would be expected to have an important role in the activation mechanism for CO oxidation.

The effects of O_{bvac} and H_a on the charge states of Au nanoclusters supported on reduced TiO_2 have been widely studied. More recently, the effects of Ti_{int} on the charge state of Au nanoclusters on reduced TiO_2 have also been investigated. A TEM study showed that Ti_{int} is found at the interface between Au and TiO_2 with a high density, suggesting that the effects of Ti_{int} on the charge states of the Au nanoclusters should be considered.[45] DFT calculations showed that Au adsorbed on TiO_2 with Ti_{int} as well as Au on TiO_2 with O_{bvac} and H_a are negatively charged.[24] In contrast, Lira *et al.* suggested that the electron transfer between the Au nanocluster and the reduced TiO_2 containing Ti_{int} is not large on the basis of PES measurements.[106] Further experimental

investigations are necessary to confirm the effects of Ti_{int} on the charge state of supported Au nanoclusters.

It should be noted that the charge states of the supported Au nanoclusters on TiO_2 are significantly affected by the reduction state (amount of defects) of TiO_2. PES and DFT studies showed that Au nanoclusters supported on oxidized TiO_2 have a positive charge.[107,108] From work on powdered catalysts, positively charged Au (cationic Au) is thought to have a crucial role in the reaction mechanism of CO oxidation on Au nanoclusters supported on TiO_2.[109] Positively charged Au would be produced by changing the reduction states of TiO_2.

6. Outlook

In this account, the current knowledge and issues of debate concerning the electronic structure and manipulation mechanisms of the atomic defects in TiO_2, as well as their interaction with Au nanoclusters, are described. Regarding the electronic structure, the spatial distribution and origin of the BGSs are still under debate. In particular, information regarding the true nature of Ti_{int} is lacking. As described above, the direct observation of the electronic structure in the subsurface or bulk region would provide decisive conclusions. The manipulation mechanisms of the atomic defects of TiO_2 have not been well investigated. Elucidating the mechanisms of the underlying reactions would allow for alignment control to create new functionality for the metal oxides. Several investigations on the manipulation of adsorbed atoms or molecules have been reported.[110–112] Therefore, the manipulation mechanisms of atomic defects may be elucidated in the near future. Regarding the interaction of atomic defects with Au nanoclusters, I personally believe that it has been confirmed that Au supported on reduced TiO_2 is negatively charged. The role of the charge state of Au nanoclusters under catalytic conditions has been investigated; however, it remains controversial.[94] Thus, more investigation is required to determine the role of the charge state of Au nanoclusters in a catalytic reaction.

The atomic defects on rutile TiO_2(110) are mainly discussed in this account; however, the atomic defects on the other facets of rutile TiO_2 or anatase TiO_2 should be clarified in the future. Recently, the nature of such atomic defects has been reported. For example, BGSs have been observed on the (011)-(2 × 1)[113] and (100)[114] surfaces of rutile TiO_2 as well as the (110) surface, although the detailed electronic structures were not investigated. Furthermore, the BGSs of the (101) and (001) surfaces of anatase TiO_2

have been observed at approximately 1.0 eV.[115,116] Interestingly, Moser *et al*. observed dispersive behavior of the defect states at 0.1 eV on anatase (001) that is different from rutile using ARPES,[117] suggesting that the behaviors of the BGSs on the anatase and rutile TiO_2 surfaces are different. The characteristic nature of the atomic defects on the other facets of rutile TiO_2 and anatase TiO_2 need to be investigated.

In addition to the defects that are currently known and investigated, such as oxygen vacancies, atomic hydrogen, and interstitial Ti, it is expected that new types of atomic defects will be discovered. If the introduction of metal vacancies or interstitial oxygen could be controlled, it would lead to new functionalities. The oxygen vacancies, atomic hydrogen and interstitial Ti in TiO_2 confer n-type semiconducting properties by producing excess electrons. The introduction of metal vacancies or interstitial oxygen would result in holes in TiO_2, leading to novel characteristics.

Finally, clarification of the physical properties of atomic defects in TiO_2 is needed for applications related to chemical reactions and device performance. With respect to the functionality of TiO_2, it should be possible to control the reaction sites for catalytic and photocatalytic reactions by controlling the distribution of electrons and holes via defect alignment. Furthermore, defect alignment can also be used to control the routes for molecular diffusion and the transfer of electrons/holes/ions to the surface. A recent study reported the effects of defect alignment on the diffusion of alcohol and water.[118,119] The techniques used in these instances should find application in molecular and electronic devices such as batteries and fuel cells as well. To apply the knowledge obtained from surface science works, the behavior of the atomic defects in ambient or liquid conditions will be important. The recent developments in experimental techniques and theoretical calculations elucidate new aspects of TiO_2 that

could not be observed under UHV conditions.[120–127] Surface science studies in ambient or liquid conditions will demonstrate the true nature of atomic defects for application conditions.

REFERENCES

[1] As accessed on the website: http://apps.webofknowledge.com.

[2] V. E. Henrich, P. A. Cox, *The Surface Science of Metal Oxides*, Cambridge University Press, Cambridge, **1994**.

[3] A. L. Linsebigler, G. Lu, J. T. Yates Jr., *Chem. Rev.* **1995**, *95*, 735–758.

[4] U. Diebold, *Surf. Sci. Rep.* **2003**, *48*, 53–229.

[5] T. L. Thompson, J.T. Yates Jr., *Top. Catal.* **2005**, *35*, 197–210.

[6] T. L. Thompson, J. T. Yates Jr., *Chem. Rev.* **2006**, *106*, 4428–4453.

[7] J. Zhao, B. Li, K. Onda, M. Feng, H. Petek, *Chem. Rev.* **2006**, *106*, 4402–4427.

[8] C. L. Pang, R. Lindsay, G. Thornton, *Chem. Soc. Rev.* **2008**, *37*, 2328–2353.

[9] Z. Dohnalek, I. Lyubinetsky, R. Rousseau, *Prog. Surf. Sci.* **2010**, *85*, 161–205.

[10] M. A. Henderson, *Surf. Sci. Rep.* **2011**, *66*, 185–297.

[11] S. Shaikhutdinov, H.-J. Freund, *Annu. Rev. Phys. Chem.* **2012**, *63*, 619–633.

[12] A. G. Thomas, K. L. Syres, *Chem. Soc. Rev.* **2012**, *41*, 4207–4217.

[13] Z. Zhang, J. T. Yates Jr., *Chem. Rev.* **2012**, *112*, 5520–5551.

[14] M. A. Henderson, I. Lyubinetsky, *Chem. Rev.* **2013**, *113*, 4428–4455.

[15] C. L. Pang, R. Lindsay, G. Thornton, *Chem. Rev.* **2013**, *113*, 3887–3948.

[16] S. Wendt, R. Schaub, J. Matthiesen, E. K. Vestergaard, E. Wahlstrom, M. D. Rasmussen, P. Thostrup, L. M. Molina, E. Lægsgaard, I. Stensgaard, B. Hammer, F. Besenbacher, *Surf. Sci.* **2005**, *598*, 226–245.

[17] O. Bikondoa, C. L. Pang, R. Ithnin, C. A. Muryn, H. Onishi, G. Thornton, *Nat. Mater.* **2006**, *5*, 189–192.

[18] S. Kajita, T. Minato, H. S. Kato, M. Kawai, T. Nakayama, *J. Chem. Phys.* **2007**, *127*, 104709.

[19] M. Aono, R. R. Hasiguti, *Phys. Rev. B* **1993**, *48*, 12406–12414.

[20] E. Yagi, R. R. Hasiguti, M. Aono, *Phys. Rev. B* **1996**, *54*, 7945–7956.

[21] M. A. Henderson,W. S. Epling, C. L. Perkins, C. H. F. Peden, U. Diebold, *J. Phys. Chem. B* **1999**, *103*, 5328–5337.

[22] S. Wendt, P. T. Sprunger, E. Lira, G. K. H. Madsen, Z. S. Li, J. O. Hansen, J. Matthiesen, A. Blekinge-Rasmussen, E. Laegsgaard, B. Hammer, F. Besenbacher, *Science* **2008**, *320*, 1755–1759.

[23] N. Shibata, A. Goto, S.-Y. Choi, T. Mizoguchi, S. D. Findlay, T. Yamamoto, Y. Ikuhara, *Science* **2008**, *322*, 570–573.

[24] G. K. H. Madsen, B. Hammer, *J. Chem. Phys.* **2009**, *130*, 044704.

[25] E. Finazzi, C. Di Valentin, G. Pacchioni, *J. Phys. Chem. C* **2009**, *113*, 3382–3385.

[26] D. Sporleder, D. P. Wilson, M. G. White, *J. Phys. Chem. C* **2009**, *113*, 13180–13191.

[27] M. Bowker, R. A. Bennett, *J. Phys.: Condens. Matter* **2009**, *21*, 474224.

[28] E. J. Sanville, L. J. Vernon, S. D. Kenny, R. Smith, Y. Moghaddam, C. Browne, P. Mulheran, *Phys. Rev. B* **2009**, *80*, 235308.

[29] C. Di Valentin, G. Pacchioni, A. Selloni, *J. Phys. Chem. C* **2009**, *113*, 20543–20552.

[30] P. A. Mulheran, M. Nolan, C. S. Browne, M. Basham, E. Sanvillee, R. A. Bennett, *Phys. Chem. Chem. Phys.* **2010**, *12*, 9763–9771.

[31] Z. Zhang, J. Lee, J. T. Yates Jr., R. Bechstein, E. Lira, J. O. Hansen, S. Wendt, F. Besenbacher, *J. Phys. Chem. C* **2010**, *114*, 3059–3062.

[32] N. A. Deskins, R. Rousseau, M. Dupuis, *J. Phys. Chem. C* **2010**, *114*, 5891–5897.

[33] L. Benz, J. Haubrich, S. C. Jensen, C. M. Friend, *ACS Nano* **2011**, *5*, 834–843.

[34] L. Vernon, S. D. Kenny, R. Smith, E. Sanville, *Phys. Rev. B* **2011**, *83*, 075412.

[35] A. T. Brant, S. Yang, N. C. Giles, L. E. Halliburton, *J. Appl. Phys.* **2011**, *110*, 053714.

[36] C. Scott, S. Blackwell, L. Vernon, S. Kenny, M. Walls, R. Smith, *J. Chem. Phys.* **2011**, *135*, 174706.

[37] J. Zhang, A. N. Alexandrova, *J. Chem. Phys.* **2011**, *135*, 174702.

[38] E. Lira, P. Huo, J. O. Hansen, F. Rieboldt, R. Bechstein, Y. Wei, R. Streber, S. Porsgaard, Z. Li, E. Laegsgaard, S. Wendt, F. Besenbacher, *Catal. Today* **2012**, *182*, 25–38.

[39] A. Tilocca, A. Selloni, *J. Phys. Chem. C* **2012**, *116*, 9114–9121.

[40] E. Mete, O. Gulseren, S. Ellialtioglu, *Eur. Phys. J. B* **2012**, *85*, 204.

[41] H.-Y. Lee, S. J. Clark, J. Robertson, *Phys. Rev. B* **2012**, *86*, 075209.

[42] M. Chiesa, M. C. Paganini, S. Livraghi, E. Giamello, *Phys. Chem. Chem. Phys.* **2013**, *15*, 9435–9447.

[43] S. C. Jensen, C. M. Friend, *Top. Catal.* **2013**, *56*, 1377–1388.

[44] B. Santara, P. K. Giri, K. Imakita, M. Fujii, *J. Phys. Chem. C* **2013**, *117*, 23402–23411.

[45] T. Tanaka, A. Sumiya, H. Sawada, Y. Kondo, K. Takayanagi, *Surf. Sci.* **2014**, *619*, 39–43.

[46] X. Mao, X. Lang, Z. Wang, Q. Hao, B. Wen, Z. Ren, D. Dai, C. Zhou, L.-M. Liu, X. Yang, *J. Phys. Chem. Lett.* **2013**, *4*, 3839–3844.

[47] T. Minato, Y. Sainoo, Y. Kim, H. S. Kato, K.-i. Aika, M. Kawai, J. Zhao, H. Petek, T. Huang, W. He, B. Wang, Z. Wang, Y. Zhao, J. L. Yang, J. G. Hou, *J. Chem. Phys.* **2009**, *130*, 124502.

[48] S. Wendt, J. Matthiesen, R. Schaub, E. K. Vestergaard, E. Laegsgaard, F. Besenbacher, B. Hammer, *Phys. Rev. Lett.* **2006**, *96*, 066107.

[49] S. Suzuki, K. Fukui, H. Onishi, Y. Iwasawa, *Phys. Rev. Lett.* **2000**, *84*, 2156–2159.

[50] T. Minato, M. Kawai, Y. Kim, *J. Mater. Res.* **2012**, *27*, 2237–2240.

[51] T. Minato, N. Asao, Y. Yamamoto, M. Kawai, Y. Kim, *Chem. Lett.* **2013**, *42*, 942–943.

[52] K. Fukui, H. Onishi, Y. Iwasawa, *Phys. Rev. Lett.* **1997**, *79*, 4202–4205.

[53] A. Yurtsever, D. Fernandez-Torre, C. Gonzalez, P. Jelinek, P. Pou, Y. Sugimoto, M. Abe, R. Perez, S. Morita, *Phys. Rev. B* **2012**, *85*, 125416.

[54] R. Schaub, P. Thostrup, N. Lopez, E. Laegsgaard, I. Stensgaard, J. K. Norskov, F. Besenbacher, *Phys. Rev. Lett.* **2001**, *87*, 266104.

[55] R. Schaub, *Science* **2006**, *314*, 925.

[56] V. E. Henrich, G. Dresselhaus, H. J. Zeiger, *Phys. Rev. Lett.* **1976**, *36*, 1335–1339.

[57] W. Gopel, J. A. Anderson, D. Frankel, M. Jaehnig, K. Phillips, J. A. Schafer, G. Rocker, *Surf. Sci.* **1984**, *139*, 333–346.

[58] Y. Aiura, Y. Nishihara, Y. Haruyama, T. Komeda, S. Kodaira, Y. Sakisaka, T. Maruyama, H. Kato, *Phys. B* **1994**, *194–196*, 1215–1216.

[59] M. Tsukada, C. Satoko, H. Adachi, *J. Phys. Soc. Jpn.* **1979**, *47*, 1610–1619.

[60] C. R. Wang, Y. S. Xu, *Surf. Sci.* **1989**, *219*, L537–L542.

[61] C. Di Valentin, G. Pacchioni, A. Selloni, *Phys. Rev. Lett.* **2006**, *97*, 166803.

[62] T. Bredow, G. Pacchioni, *Chem. Phys. Lett.* **2002**, *355*, 417–423.

[63] A. Vijay, G. Mills, H. Metiu, *J. Chem. Phys.* **2003**, *118*, 6536–6551.

[64] A.T. Paxton, L. Thien-Nga, *Phys. Rev. B* **1998**, *57*, 1579–1584.

[65] M. A. Henderson,W. S. Epling, C. L. Perkins, C. H. F. Peden, U. Diebold, *J. Phys. Chem. B* **1999**, *103*, 5328–5337.

[66] P. Krüger, S. Bourgeois, B. Domenichini, H. Magnan, D. Chandesris, P. Le Fevre, A. M. Flank, J. Jupille, L. Floreano, A. Cossaro, A. Verdini, A. Morgante, *Phys. Rev. Lett.* **2008**, *100*, 055501.

[67] A. C. Papageorgiou, N. S. Beglitis, C. L. Pang, G. Teobaldi, G. Cabailh, Q. Chen, A. J. Fisher, W. A. Hofer, G. Thornton, *Proc. Natl. Acad. Sci. U. S. A.* **2010**, *107*, 2391–2396.

[68] N. A. Deskins, R. Rousseau, M. Dupuis, *J. Phys. Chem. C* **2011**, *115*, 7562–7572.

[69] S. Chretien, H.Metiu, *J. Phys. Chem.C***2011**, *115*, 4696–4705.

[70] N. A. Deskins, M. Dupuis, *Phys. Rev. B* **2007**, *75*, 195212.

[71] Y. Cai, Z. Bai, S. Chintalapati, Q. Zeng, Y. P. Feng, *J. Chem. Phys.* **2013**, *138*, 154711.

[72] C. M. Yim, C. L. Pang, G. Thornton, *Phys. Rev. Lett.* **2010**, *104*, 036806.

[73] K. Mitsuhara, H. Okumura, A. Visikovskiy, M. Takizawa, Y. Kido, *J. Chem. Phys.* **2012**, *136*, 124707.

[74] L. E. Walle, A. Borg, P. Uvdal, A. Sandell, *Phys. Rev. B* **2012**, *86*, 205415.

[75] It has also been reported that CH_3 on O_b formed by the dissociation of methanol on O_{bvac} has a contribution to the BGSs as well as atomic H.[46]

[76] M. L. Knotek, P. J. Feibelman, *Phys. Rev. Lett.* **1978**, *40*, 964–967.

[77] Z. Zhang, K. Cao, J. T. Yates Jr., *J. Phys. Chem. Lett.* **2013**, *4*, 674–679.

[78] M. Lastapis, M. Martin, D. Riedel, L. Hellner, G. Comtet, G. Dujardin, *Science* **2005**, *308*, 1000–1003.

[79] B. C. Stipe, M. A. Rezaei, W. Ho, *Science* **1998**, *279*, 1907–1909.

[80] T.-C. Shen, C. Wang, G. C. Abeln, J. R. Tucker, J.W. Lyding, Ph. Avouris, R. E. Walkup, *Science* **1995**, *268*, 1590–1592.

[81] T. Komeda, Y. Kim, M. Kawai, B. N. J. Persson, H. Ueba, *Science* **2002**, *295*, 2055–2058.

[82] D. M. Eigler, C. P. Lutz, W. E. Rudge, *Nature* **1991**, *352*, 600–603.

[83] J. K. Gimzewski, C. Joachim, *Science* **1999**, *283*, 1683–1688.

[84] J. M. Carpinelli, B. S. Swartzentruber, *Phys. Rev. B* **1998**, *58*, R13423–R13425.

[85] Y. W. Mo, *Science* **1993**, *261*, 886–888.

[86] M. Alemani, M. V. Peters, S. Hecht, K.-H. Rieder, F. Moresco, L. Grill, *J. Am. Chem. Soc.* **2006**, *128*, 14446–14447.

[87] U. Diebold, J. Lehman, T. Mahmoud, M. Kuhn, G. Leonardelli, W. Hebenstreit, M. Schmid, P. Varga, *Surf. Sci.***1998**, *411*, 137–153.

[88] D. P. Acharya, C. V. Ciobanu, N. Camillone, P. Sutter, *J. Phys. Chem. C* **2010**, *114*, 21510–21515.

[89] X. Cui, B. Wang, Z. Wang, T. Huang, Y. Zhao, J. L. Yang, J. G. Hou, *J. Chem. Phys.* **2008**, *129*, 044703.

[90] M. Setvin, U. Aschauer, P. Scheiber, Y.-F. Li, W. Y. Hou, M. Schmid, A. Selloni, U. Diebold, *Science* **2013**, *341*, 988–991.

[91] T. Minato, Y. Izumi, K.-i. Aika, A. Ishiguro, T. Nakajima, Y. Wakatsuki, *J. Phys. Chem. B* **2003**, *107*, 9022–9028.

[92] M. Haruta, S. Tsubota, T. Kobayashi, H. Kageyama, M. J. Genet, B. Delmon, *J. Catal.* **1993**, *144*, 175–192.

[93] M. Haruta, *Gold Bull.* **2004**, *37*, 27–36.

[94] J. Gong, *Chem. Rev.* **2012**, *112*, 2987–3054.

[95] E. C. H. Sykes, F. J. Williams, M. S. Tikhov, R. M. Lambert, *J. Phys. Chem. B* **2002**, *106*, 5390–5394.

[96] E. Wahlstrom, N. Lopez, R. Schaub, P. Thostrup, A. Ronnau, C. Africh, E. Laegsgaard, J. K. Norskov, F. Besenbacher, *Phys. Rev. Lett.* **2003**, *90*, 026101.

[97] T. Minato, T. Susaki, S. Shiraki, H. S. Kato, M. Kawai, K. Aika, *Surf. Sci.* **2004**, *566–568*, 1012–1017.

[98] M. S. Chen, D. W. Goodman, *Science* **2004**, *306*, 252–255.

[99] A. S. Wörz, U. Heiz, F. Cinquini, G. Pacchioni, *J. Phys. Chem. B* **2005**, *109*, 18418–18426.

[100] M. Okumura, Y. Kitagawa, M. Haruta, K. Yamaguchi, *Appl. Catal., A* **2005**, *291*, 37–44.

[101] J. D. Stiehl, T. S. Kim, S. M. McClure, C. B. Mullins, *J. Am. Chem. Soc.* **2004**, *126*, 1606–1607.

[102] J. D. Stiehl, J. L. Gong, R. A. Ojifinni, T. S. Kim, S. M. McClure, C. B. Mullins, *J. Phys. Chem. B* **2006**, *110*, 20337–20343.

[103] M. S. Chen, D.W. Goodman, *Catal. Today* **2006**, *111*, 22–45.

[104] Y.-G. Wang, Y. Yoon, V.-A. Glezakou, J. Li, R. Rousseau, *J. Am. Chem. Soc.* **2013**, *135*, 10673–10683.

[105] H. J. Chung, A. Yurtsever, Y. Sugimoto, M. Abe, S. Morita, *Appl. Phys. Lett.* **2011**, *99*, 123102.

[106] E. Lira, J. Ø. Hansen, L. R. Merte, P. T. Sprunger, Z. Li, F. Besenbacher, S. Wendt, *Top. Catal.* **2013**, *56*, 1460–1476.

[107] K. Okazaki, Y.Morikawa, S. Tanaka, K. Tanaka, M. Kohyama, *Phys. Rev. B* **2004**, *69*, 235404.

[108] A. Visikovskiy, K. Mitsuhara, Y. Kido, *J. Vac. Sci. Technol., A* **2013**, *31*, 061404.

[109] G. C. Bond, D. T. Thompson, *Gold Bull.* **2000**, *33*, 41–51.

[110] Z.-T. Wang, Y. Du, Z. Dohnalek, I. Lyubinetsky, *J. Phys. Chem. Lett.* **2010**, *1*, 3524–3529.

[111] J. Lee, D. C. Sorescu, X. Deng, *J. Am. Chem. Soc.* **2011**, *133*, 10066–10069.

[112] S. J. Tan, Y. Zhao, J. Zhao, Z. Wang, C. X. Ma, A. D. Zhao, B. Wang, Y. Luo, J. L. Yang, J. G. Hou, *Phys. Rev. B* **2011**, *84*, 155418.

[113] T. J. Beck, A. Klust, M. Batzill, U. Diebold, C. Di Valentin, A. Tilocca, A. Selloni, *Surf. Sci.* **2005**, *591*, L267–L272.

[114] C. A. Muryn, P. J. Hardman, J. J. Crouch, G. N. Raiker, G. Thornton, D. S. L. Law, *Surf. Sci.* **1991**, *251–252*, 747–752.

[115] A. G. Thomas, W. R. Flavell, A. K. Mallick, A. R. Kumarasinghe, D. Tsoutsou, N. Khan, C. Chatwin, S. Rayner, G. C. Smith, R. L. Stockbauer, S.Warren, T. K. Johal, S. Patel, D. Holland, A. Taleb, F. Wiame, *Phys. Rev. B* **2007**, *75*, 035105.

[116] Y. Wang, H. J. Sun, S. J. Tan, H. Feng, Z.W. Cheng, J. Zhao, A. D. Zhao, B. Wang, Y. Luo, J. L. Yang, J. G. Hou, *Nat. Commun.* **2013**, *4*, 2214–2221.

[117] S.Moser, L.Moreschini, J. Jacimovic, O. S. Barisic, H. Berger, A. Magrez, Y. J. Chang, K. S. Kim, A. Bostwick, E. Rotenberg, L. Forro, M. Grioni, *Phys. Rev. Lett.* **2013**, *110*, 196403.

[118] S.-C. Li, L.-N. Chu, X.-Q. Gong, U. Diebold, *Science* **2010**, *328*, 882–884.

[119] Y. Du, N. A. Deskins, Z. Zhang, Z. Dohnalek, M. Dupuis, I. Lyubinetsky, *Phys. Rev. Lett.* **2009**, *102*, 096102.

[120] E. Tsunemi, K. Kobayashi, N. Oyabu, M. Hirose, Y. Takenaka, K. Matsushige, H. Yamada, *Rev. Sci. Instrum.* **2013**, *84*, 083701.

[121] S. Ido, H. Kimiya, K. Kobayashi, H. Kominami, K. Matsushige, H. Yamada, *Nat. Mater.* **2014**, *13*, 264–271.

[122] K. Miyata, H. Asakawa, T. Fukuma, *Appl. Phys. Lett.* **2013**, *103*, 203104.

[123] N. Kodera, D. Yamamoto, R. Ishikawa, T. Ando, *Nature* **2010**, *468*, 72–77.

[124] Y. Yokota, H. Hara, T. Harada, A. Imanishi, T. Uemura, J. Takeya, K. I. Fukui, *Chem. Commun.* **2013**, *49*, 10596–10598.

[125] A. Taranovskyy, T. Tansel, O. M. Magnussen, *Phys. Rev. Lett.* **2010**, *104*, 106101.

[126] U. Aschauer, A. Selloni, *Phys. Rev. Lett.* **2011**, *106*, 166102.

[127] M. Sumita, C. Hu, Y. Tateyama, *J. Phys. Chem. C* **2010**, *114*, 18529–18537.

Table 1. Reviews and textbooks related to atomic defects in TiO_2.

Authors	Journal or book title	Year	Vol.	Page	Ref. number
V. E. Henrich and P. A. Cox	*The surface science of metal oxides*	**1994**			[2]
A. L. Linsebigler, G. Q. Lu and J. T. Yates	*Chem. Rev.*	**1995**	*95*	735–758	[3]
U. Diebold	*Surf. Sci. Rep.*	**2003**	*48*	53–229	[4]
T. L. Thompson and J. T. Yates	*Top. Catal.*	**2005**	*35*	197–210	[5]
T. L. Thompson and J. T. Yates	*Chem. Rev.*	**2006**	*106*	4428–4453	[6]
J. Zhao, B. Li, K. Onda, M. Feng, and H. Petek	*Chem. Rev.*	**2006**	*106*	4402–4427	[7]
C. L. Pang, R. Lindsay and G. Thornton	*Chem. Soc. Rev.*	**2008**	*37*	2328–2353	[8]
Z. Dohnalek, I. Lyubinetsky and R. Rousseau	*Prog. Surf. Sci.*	**2010**	*85*	161–205	[9]
M. A. Henderson	*Surf. Sci. Rep.*	**2011**	*66*	185–297	[10]
S. Shaikhutdinov, H.-J. Freund	*Annu. Rev. Phys. Chem.*	**2012**	*63*	619–633	[11]
A. G. Thomas and K. L. Syres	*Chem. Soc. Rev.*	**2012**	*41*	4207–4217	[12]
Z. Zhang and J. T. Yates	*Chem. Rev.*	**2012**	*112*	5520–5551	[13]
M. A. Henderson and I. Lyubinetsky	*Chem. Rev.*	**2013**	*113*	4428–4455	[14]
C. L. Pang, R. Lindsay and G. Thornton	*Chem. Rev.*	**2013**	*113*	3887–3948	[15]

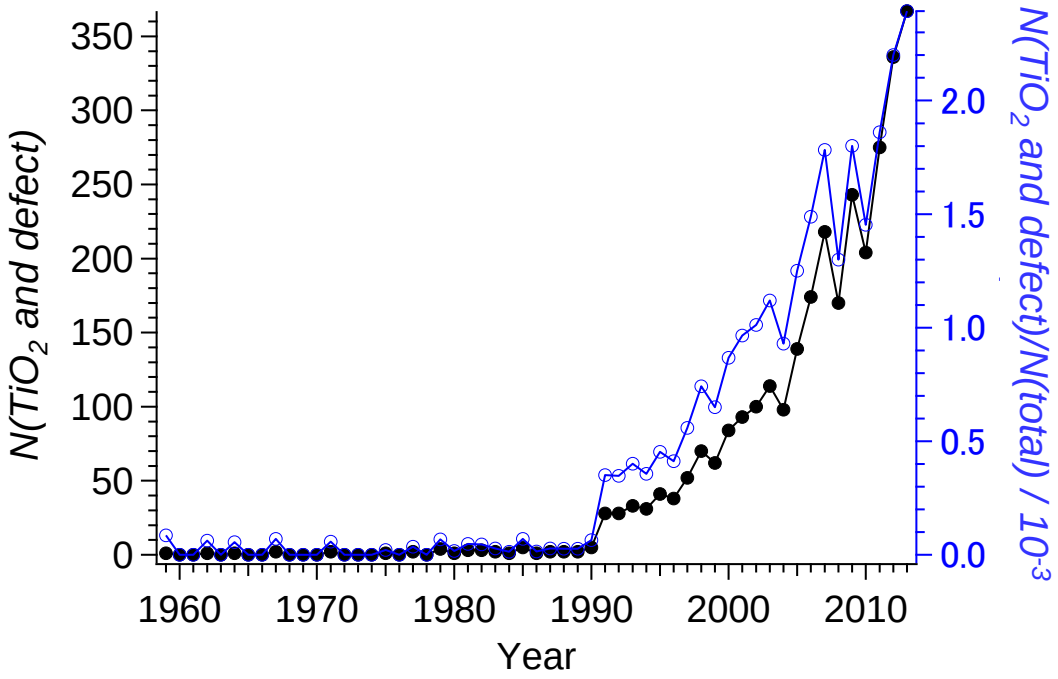

Fig 1. The black [*N(TiO$_2$ and defect*)] and blue [*N(TiO$_2$ and defect)/N(total)*] curves were determined using the Web of Science™ platform.[1] Here, *N(TiO$_2$ and defect)* and *N(total)* are the number of publications corresponding to the keywords "TiO$_2$" and "defect" and the total number of publications in all journals, respectively. Articles, letters, and reviews were included in these calculations.

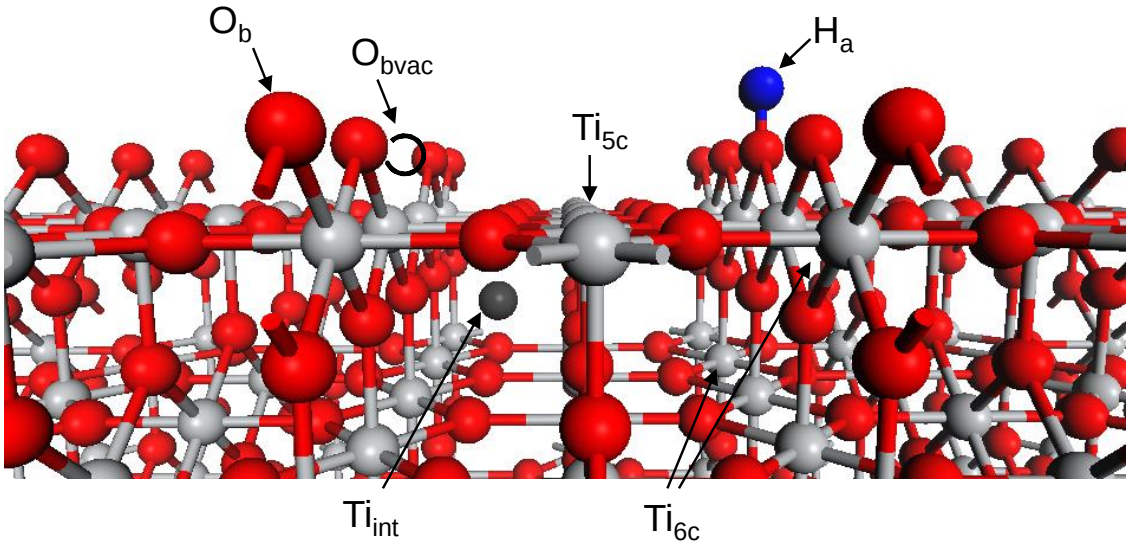

Fig. 2. Surface structure of the bridging oxygen vacancies (O_{bvac}), atomic hydrogen (H_a), and interstitial Ti (Ti_{int}) on the rutile TiO_2(110) surface. The bridging oxygen (O_b), five-coordinated Ti (Ti_{5c}), and six-coordinated Ti (Ti_{6c}) are also shown. The red and gray balls represent oxygen and titanium ions, respectively.

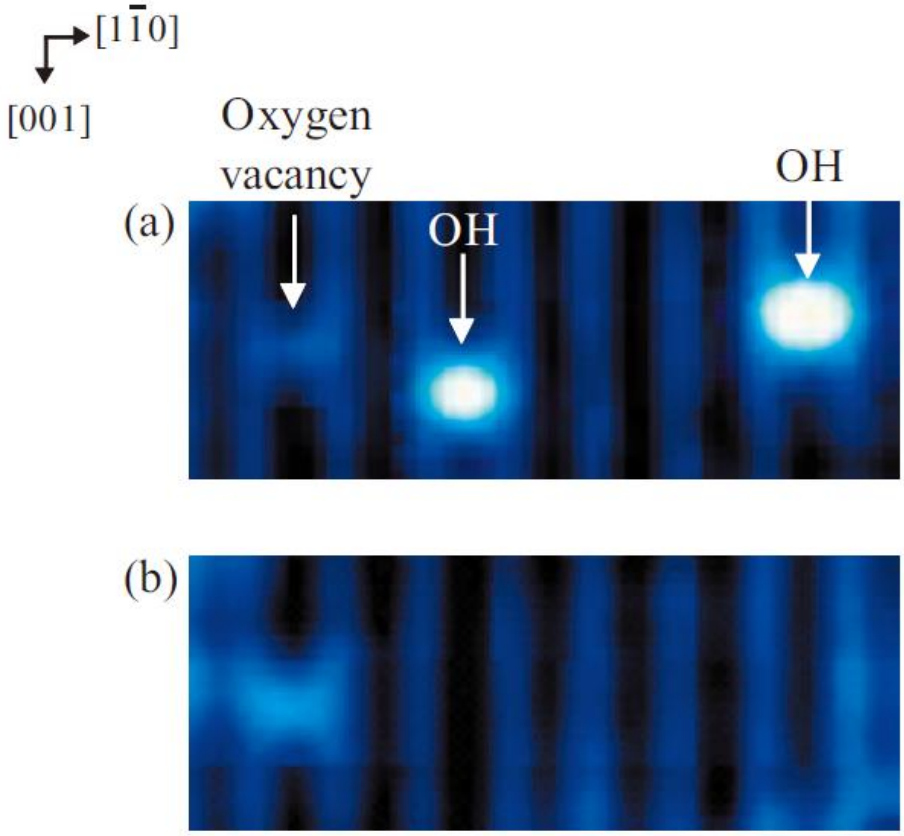

Fig. 3. 6.5 × 2.6 nm^2 constant-current STM images of H_a (OH in figure) and O_{bvac} on a rutile TiO_2(110) surface. V_{sample} = +1.5 V and I_{tunnel} = 0.3 nA at 78 K. (a) Before and (b) after scanning at V_{sample} = +3.0 V and I_{tunnel} = 0.3 nA.[47] Copyright 2009 American Institute of Physics.

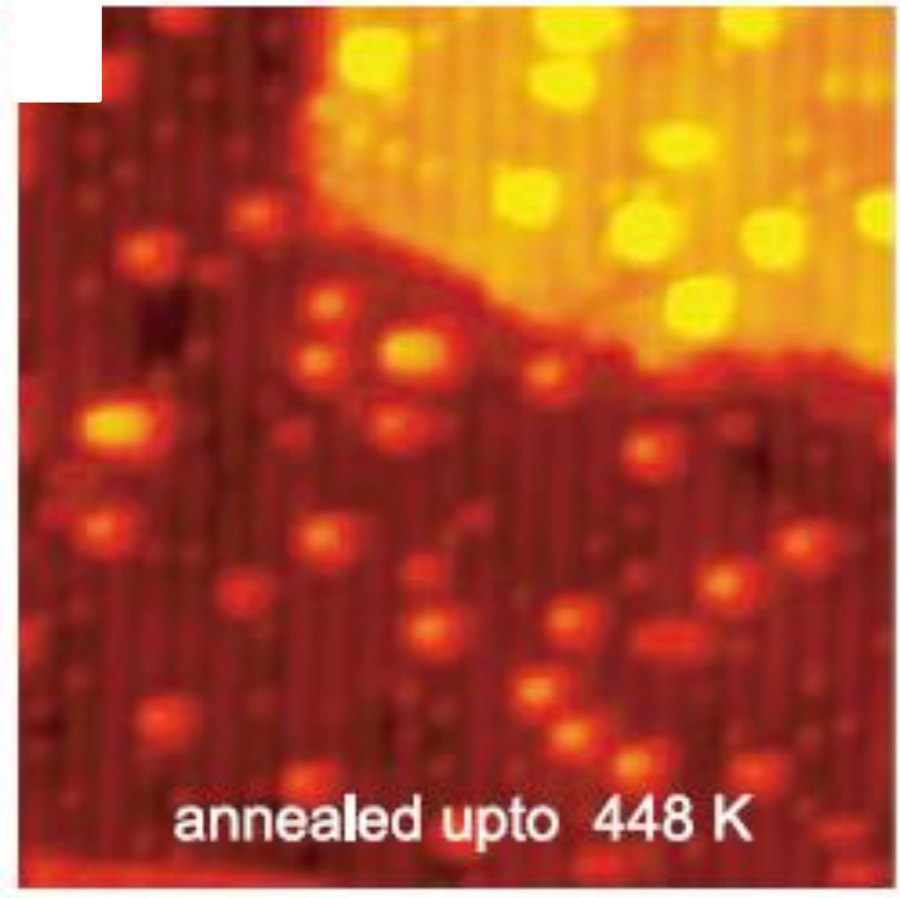

Fig. 4. 15 × 15 nm^2 STM image of a rutile TiO_2(110) surface with TiO_x formed by a reaction between Ti_{int} and oxygen molecules. Reprinted with permission from reference [22]. Copyright 2008 American Association for the Advancement of Science.

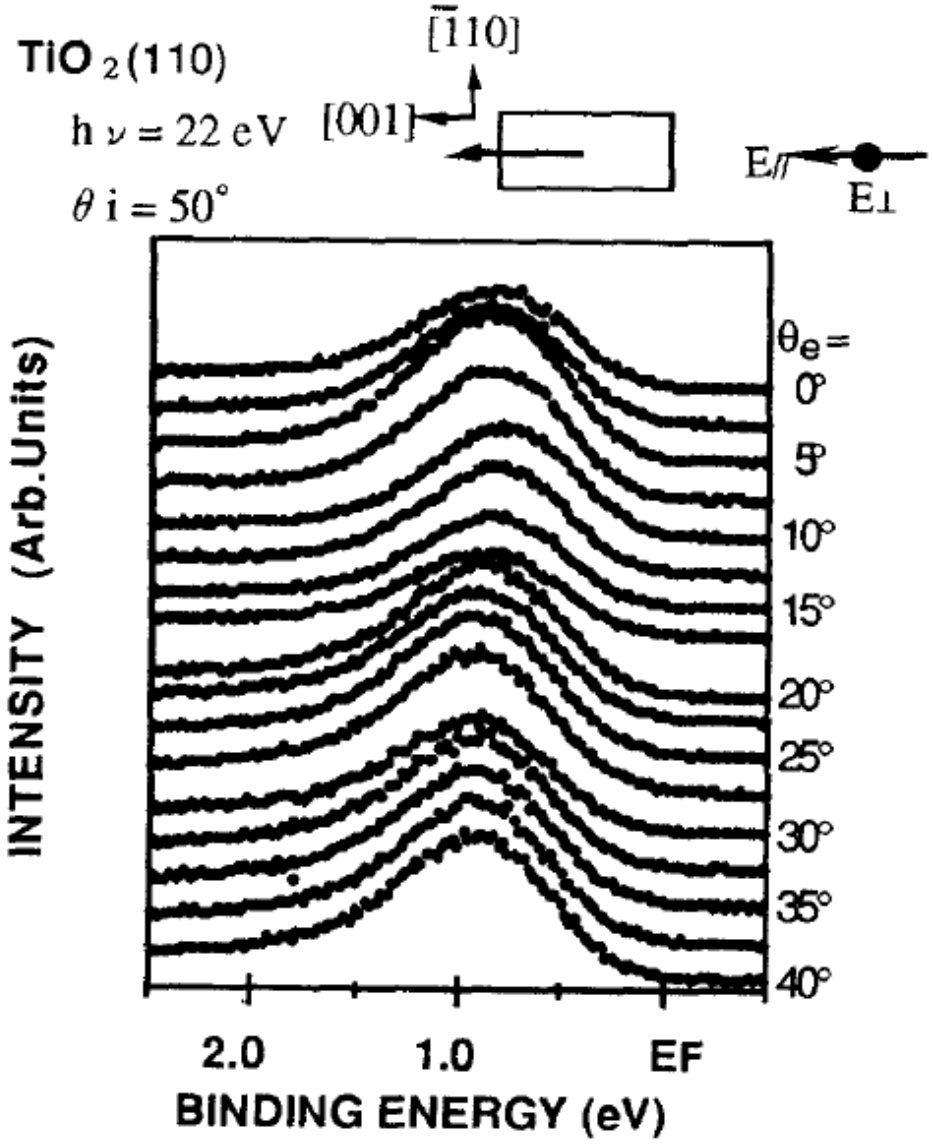

Fig. 5. ARPES spectra of a reduced TiO_2(110) surface obtained along the off-normal to the [001] direction.[58] Copyright 1994 Elsevier.

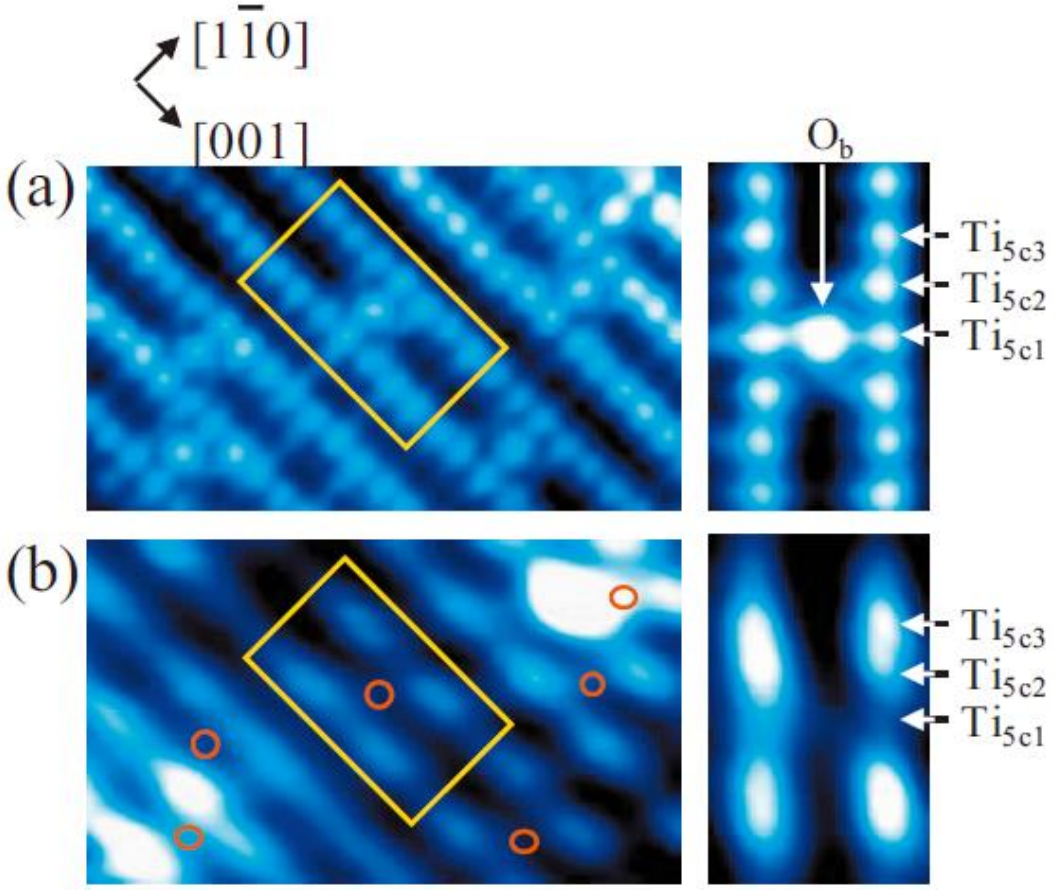

Fig. 6. 3.4 × 5.8 nm^2 constant-current STM images of O_{bvac} vacancies on a rutile TiO_2(110) surface at 78 K. (a) Unoccupied-state image (V_{sample} = +0.6 V and I_{tunnel} = 0.6 nA) observed in the forward scanning mode, and (b) occupied state image (V_{sample} = −1.1 V and I_{tunnel} = 0.1 nA) observed in the reverse scanning mode. Magnified images (2.1 × 1.3 nm^2) of the area around the O_{bvac} sites [yellow rectangles in (a) and (b)] are also shown. The open red circles indicate the positions of the O_{bvac} sites.[47] Copyright 2009 American Institute of Physics.

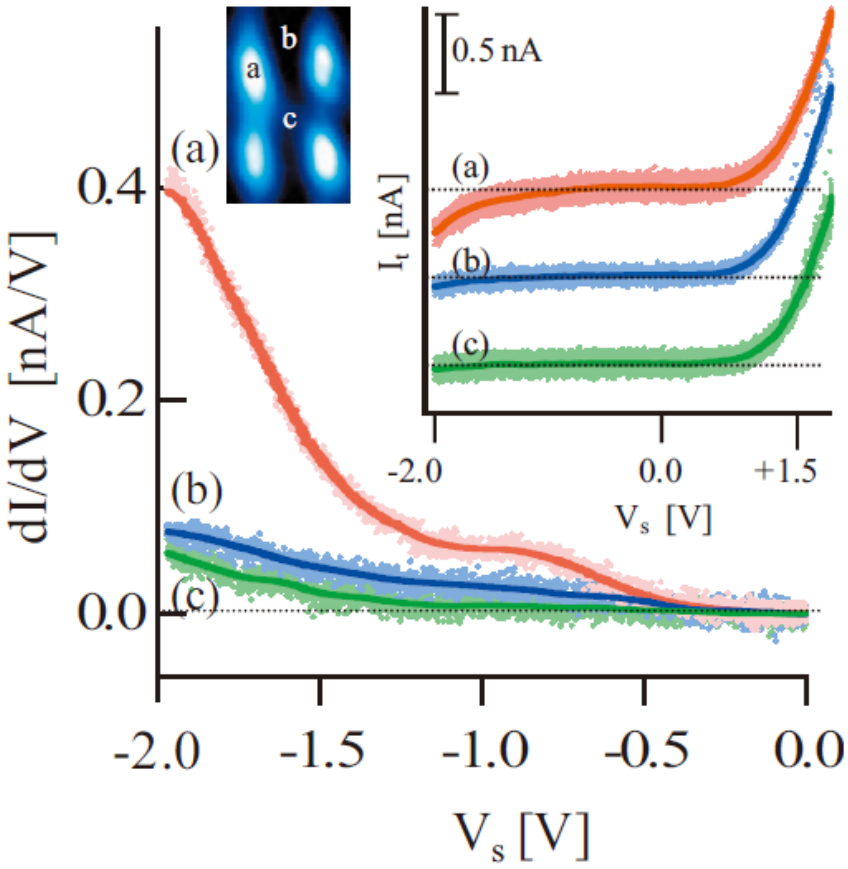

Fig. 7. STS current (*I*)–voltage (*V*) (inset) and d*I*/d*V* curves of the positiondependent occupied density of states at an O_{bvac} site. The measurement sites are indicated in the occupied-state STM image. The set-point values of *V*sample and *I*tunnel were fixed at +1.5 V and 1.0 nA, respectively.[s] Copyright 2009 American Institute of Physics.

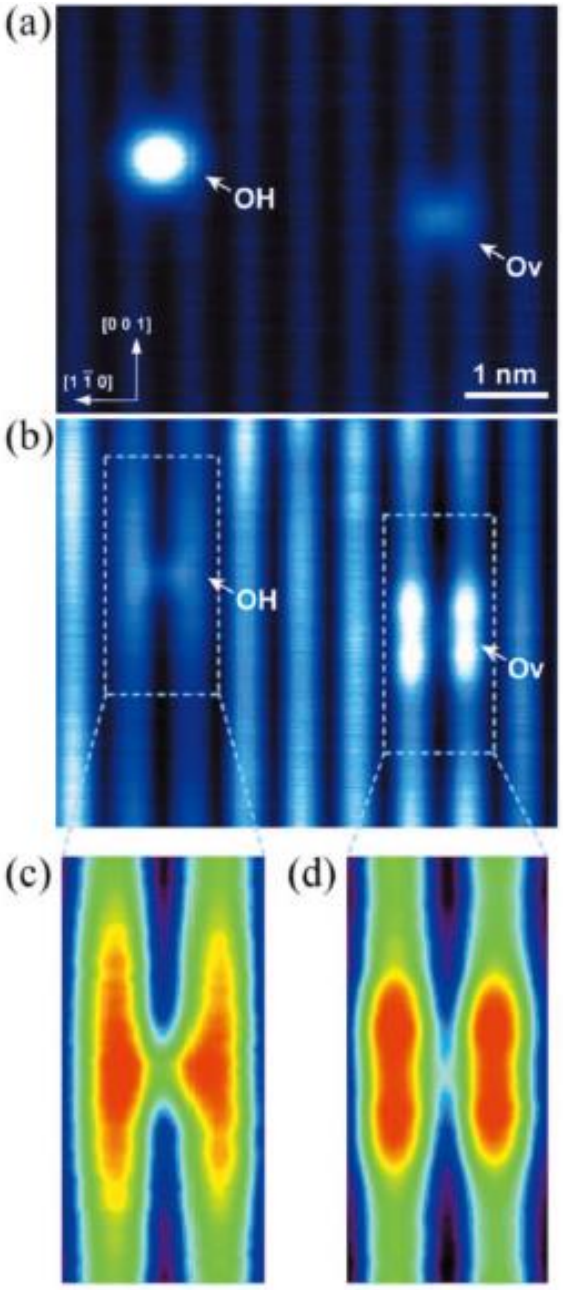

Fig. 8. (a) An unoccupied-state image at V_{sample} = +1.4 V and I_{tunnel} = 0.01 nA and (b) an occupied-state image at V_{sample} = −1.4 V and I_{tunnel} = 0.005 nA for O_{bvac} and H_a on rutile TiO_2(110) (image size: 5.8 × 6.6 nm^2, T_{sample} = 78 K). High-contrast images of (c) H_a and (d) O_{bvac}.[47] Copyright 2009 American Institute of Physics.

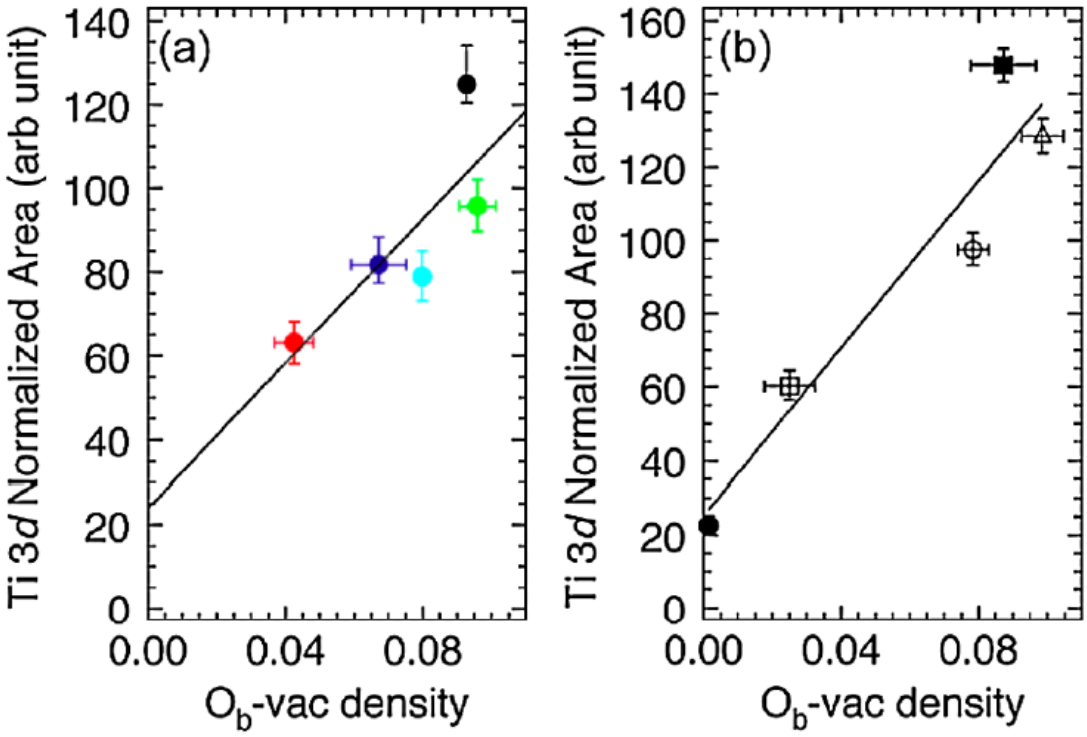

Fig. 9. Normalized integrated intensities of the band-gap states of ultraviolet photoelectron spectroscopy (UPS) peaks as functions of the O_{bvac} density on a rutile TiO_2(110) surface, determined using STM. (a) Data taken from experiments performed on TiO_2 (color of the plots indicates the different densities of the O_{bvac}. The details are described in ref. [72]). (b) Data taken from experiments performed on hydroxylated TiO_2(110). The data points are for the initially hydroxylated surface (filled square), the oxidized surface (filled circle), and the oxidized surface subjected to electron bombardment for 2 (open square), 5 (open circle), and 10 s (open triangle).[72] Reprinted with permission from reference [72]. Copyright 2010 American Physical Society (http://journals.aps.org/prl/abstract/10.1103/PhysRevLett.104.036806).

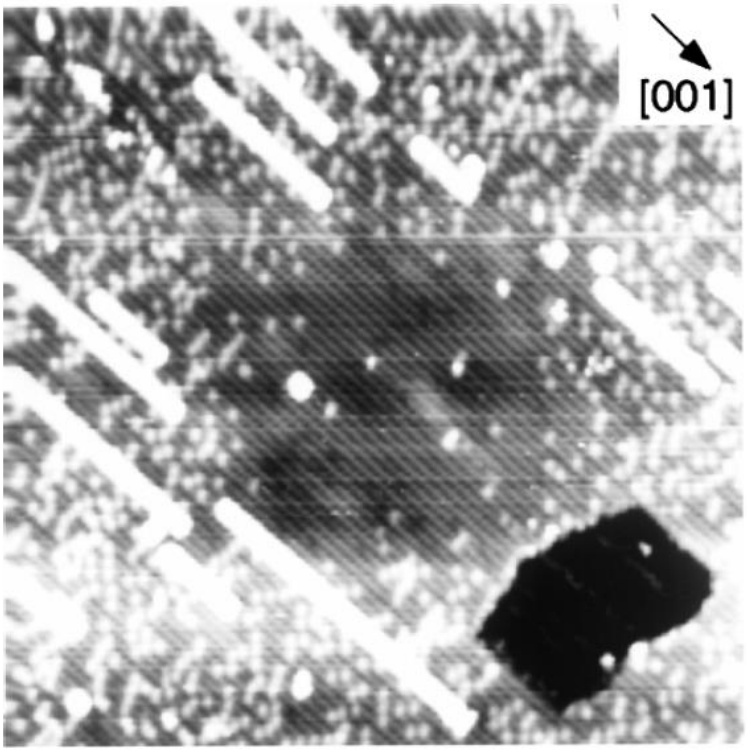

Fig. 10. STM-induced desorption of Ha on the rutile TiO_2(110) surface. The constant-current topography of the surface is shown after the high-bias scan for manipulation. Manipulation scan: 20 × 20 nm^2, V_{sample} = +3.0 V, and I_{tunnel} = 0.30 nA. Imaging scan: 50 × 50 nm^2, V_{sample} = +2.0 V, and I_{tunnel} = 0.30 nA.[49] Reprinted with permission from reference [49]. Copyright 2000 American Physical Society (http://journals.aps.org/prl/abstract/10.1103/PhysRevLett.84.2156).

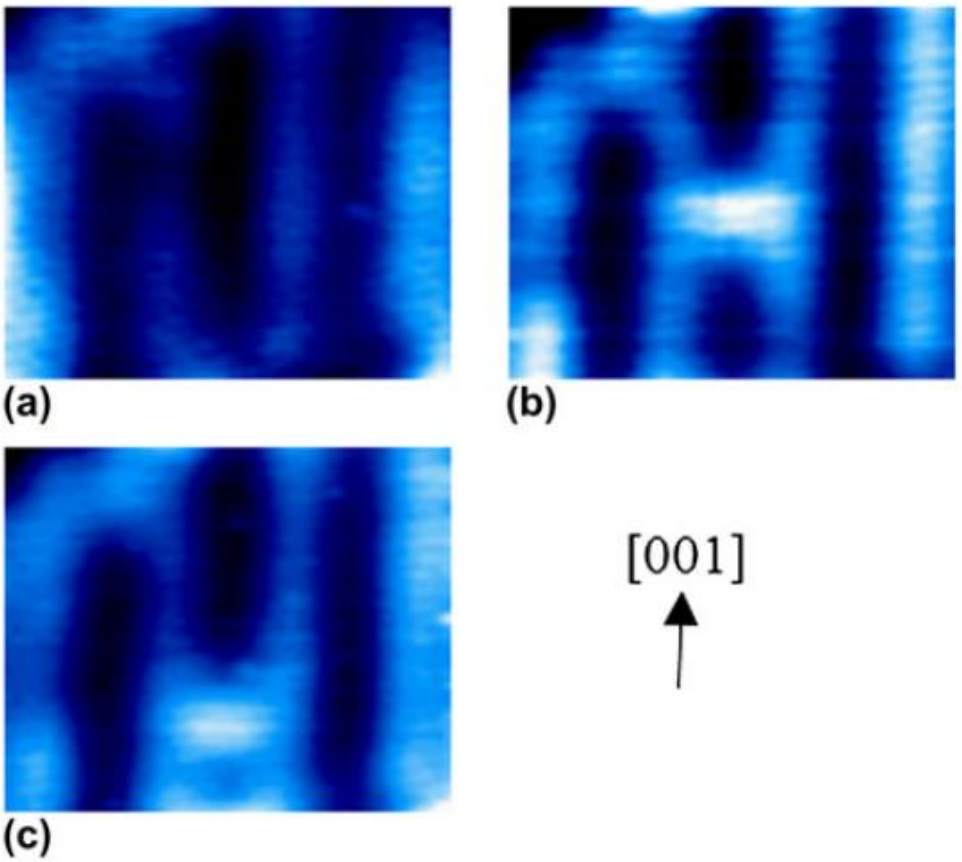

Fig. 11. Constant-current STM images of a rutile TiO_2(110) surface (a) before and (b) after pulse injection to an O_{bvac} site. (c) A constant-current STM image obtained after applying a pulse to the species that appears at the center of the STM image in (b). All STM images were obtained at V_{sample} = +1.5 V, I_{tunnel} = 0.3 nA, and T_{sample} = 78 K (3.5 × 2.9 nm^2). The applied pulses were V_{sample} = −2.0 and +4.0 V for 1 s to O_b and the species that appeared (O_{bvac}), respectively, with the feedback loop turned off.[50] Reproduced from reference [50] with permission. Copyright 2012 Cambridge University Press.

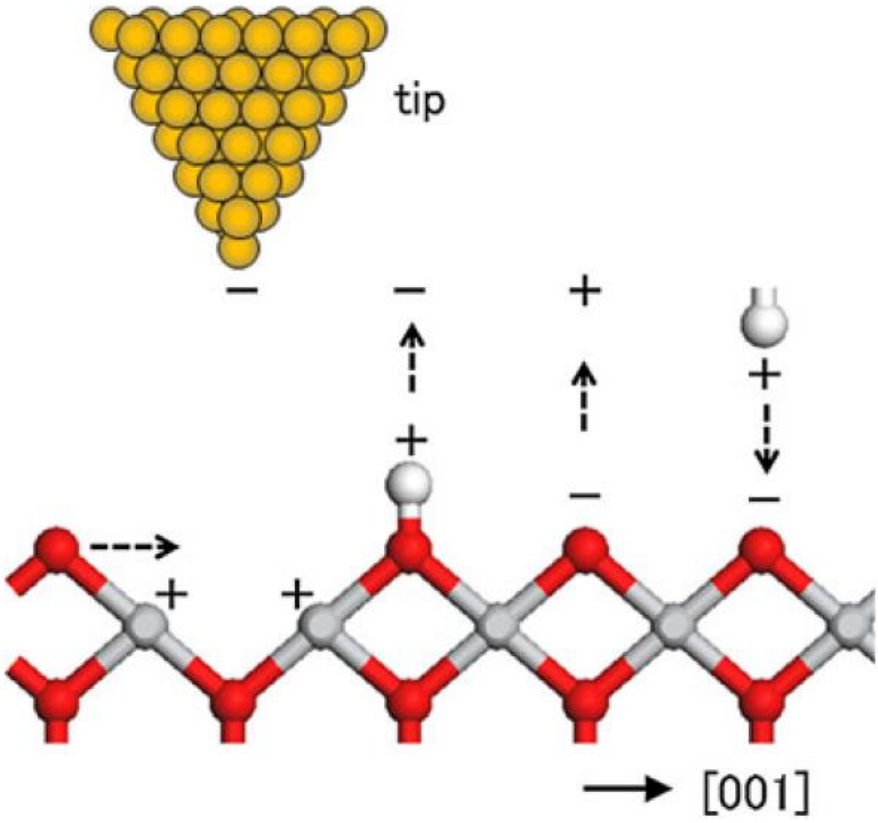

Fig. 12. A schematic image of the reactions of the atomic defects on a rutile TiO_2(110) surface with an STM tip. The gray, red, and white balls are Ti, O, and H atoms, respectively.[50] Reproduced from reference [50] with permission. Copyright 2012 Cambridge University Press.

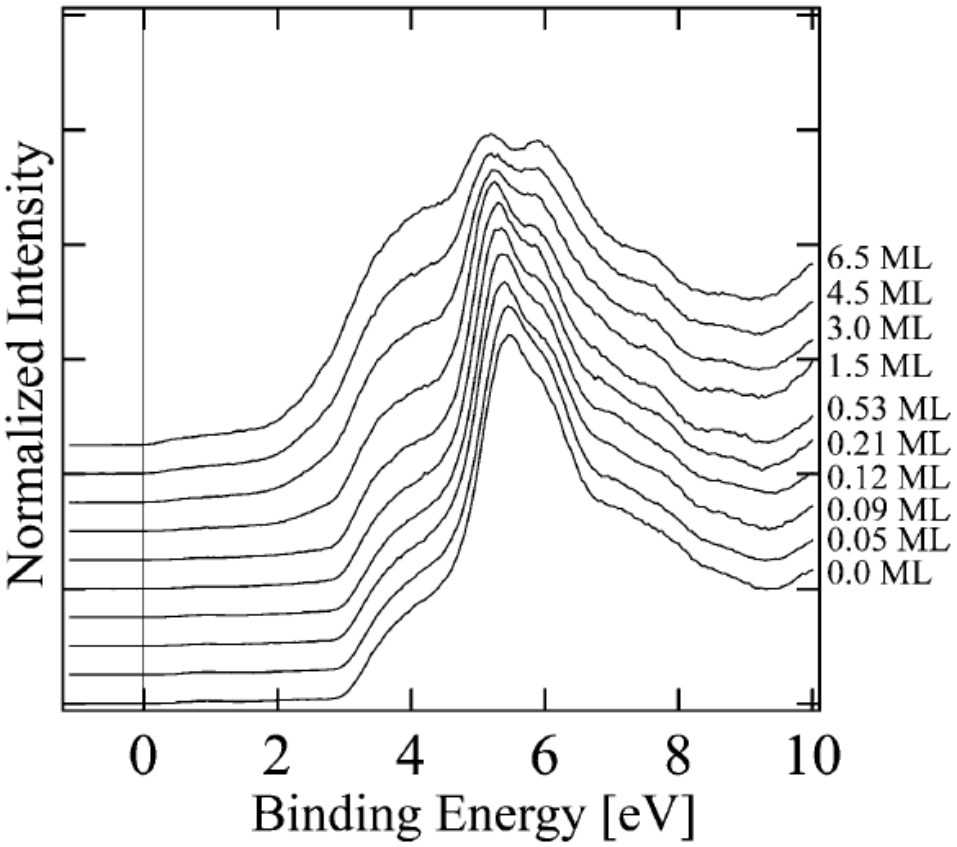

Fig. 13. PES spectra of Au/TiO_2(110) as a function of Au coverage.[97] Copyright 2004 Elsevier.

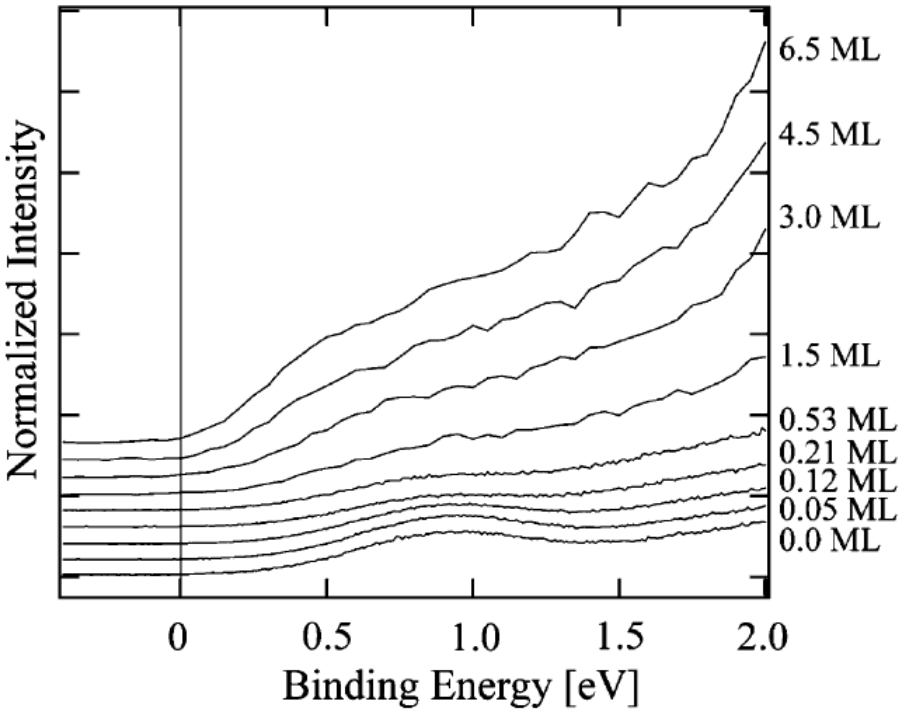

Fig. 14. PES spectra of Au/TiO_2(110) near the Fermi level as a function of Au coverage.[97] Copyright 2004 Elsevier.

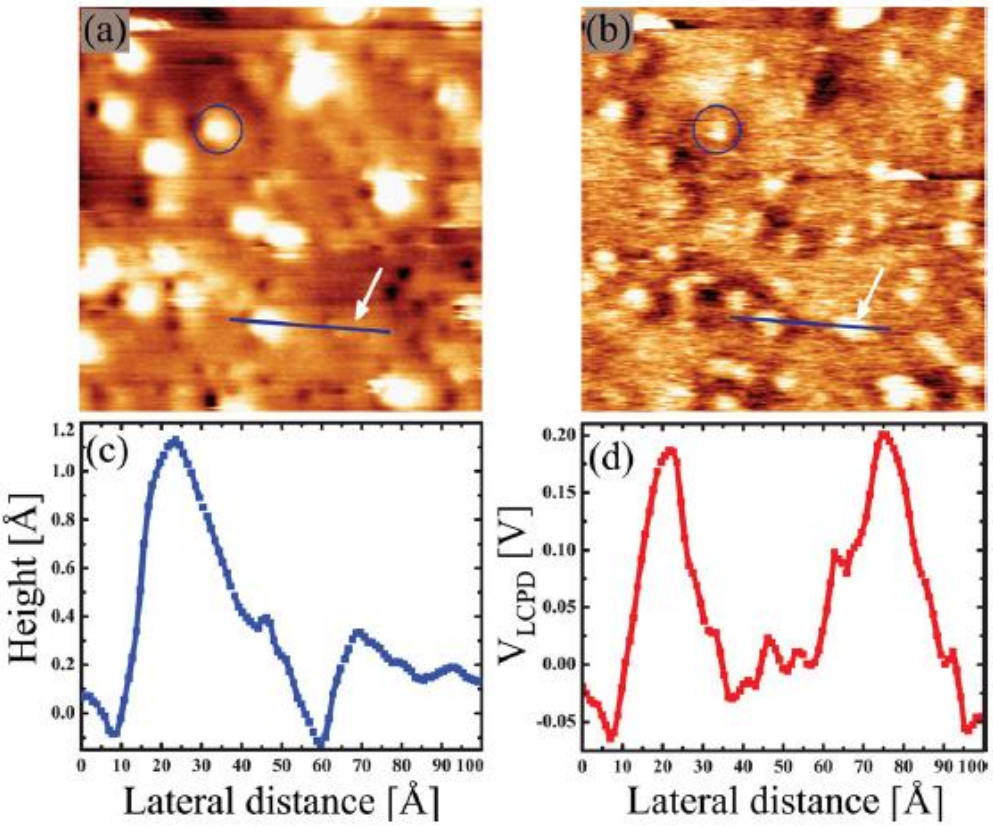

Fig. 15. Simultaneously obtained (a) non-contact atomic force microscopy topography and (b) Kelvin probe force microscopy images of Au adsorbed onto a hydroxylated rutile TiO_2(110) surface (25 × 25 nm^2). The (c) height and (d) local contact potential difference profiles were taken along the lines drawn in (a) and (b), respectively. The circles indicate Au clusters.[105] Copyright 2011 American Institute of Physics.